

Western University

Scholarship@Western

Neuroscience Institute Publications

Western Institute for Neuroscience

1-1-2022

Stratifying the Presymptomatic Phase of Genetic Frontotemporal Dementia by Serum NfL and pNfH: A Longitudinal Multicentre Study

Carlo Wilke

Hertie-Institut für klinische Hirnforschung

Selina Reich

Hertie-Institut für klinische Hirnforschung

John C. van Swieten

Erasmus MC

Barbara Borroni

Università degli Studi di Brescia

Raquel Sanchez-Valle

Universitat de Barcelona

See next page for additional authors

Follow this and additional works at: https://ir.lib.uwo.ca/neurosci_inst_pubs

Citation of this paper:

Wilke, Carlo; Reich, Selina; van Swieten, John C.; Borroni, Barbara; Sanchez-Valle, Raquel; Moreno, Fermin; Laforce, Robert; Graff, Caroline; Galimberti, Daniela; Rowe, James B.; Masellis, Mario; Tartaglia, Maria C.; Finger, Elizabeth; Vandenberghe, Rik; de Mendonça, Alexandre; Tagliavini, Fabrizio; Santana, Isabel; Ducharme, Simon; Butler, Chris R.; Gerhard, Alexander; Levin, Johannes; Danek, Adrian; Otto, Markus; Frisoni, Giovanni; Ghidoni, Roberta; Sorbi, Sandro; Bocchetta, Martina; Todd, Emily; Kuhle, Jens; and Barro, Christian, "Stratifying the Presymptomatic Phase of Genetic Frontotemporal Dementia by Serum NfL and pNfH: A Longitudinal Multicentre Study" (2022). *Neuroscience Institute Publications*. 219.

https://ir.lib.uwo.ca/neurosci_inst_pubs/219

Authors

Carlo Wilke, Selina Reich, John C. van Swieten, Barbara Borroni, Raquel Sanchez-Valle, Fermin Moreno, Robert Laforce, Caroline Graff, Daniela Galimberti, James B. Rowe, Mario Masellis, Maria C. Tartaglia, Elizabeth Finger, Rik Vandenberghe, Alexandre de Mendonça, Fabrizio Tagliavini, Isabel Santana, Simon Ducharme, Chris R. Butler, Alexander Gerhard, Johannes Levin, Adrian Danek, Markus Otto, Giovanni Frisoni, Roberta Ghidoni, Sandro Sorbi, Martina Bocchetta, Emily Todd, Jens Kuhle, and Christian Barro

Stratifying the Presymptomatic Phase of Genetic Frontotemporal Dementia by Serum NfL and pNfH: A Longitudinal Multicentre Study

Carlo Wilke, MD ^{1,2} Selina Reich, MSc,^{1,2} John C. van Swieten, MD, PhD,³ Barbara Borroni, MD, PhD ⁴ Raquel Sanchez-Valle, MD,⁵ Fermin Moreno, MD, PhD,^{6,7} Robert Laforce, MD, PhD ⁸ Caroline Graff, MD, PhD,^{9,10} Daniela Galimberti, PhD ^{11,12} James B. Rowe, MD, PhD,¹³ Mario Masellis, MD, PhD,¹⁴ Maria C. Tartaglia, MD,¹⁵ Elizabeth Finger, MD ¹⁶ Rik Vandenberghe, MD, PhD,^{17,18,19} Alexandre de Mendonça, MD, PhD,²⁰ Fabrizio Tagliavini, MD,²¹ Isabel Santana, MD, PhD,^{22,23} Simon Ducharme, MD, MSc ^{24,25} Chris R. Butler, MD,^{26,27} Alexander Gerhard, MD,^{28,29} Johannes Levin, MD,^{30,31,32} Adrian Danek, MD ³⁰ Markus Otto, MD ^{33,34} Giovanni Frisoni, MD, PhD,³⁵ Roberta Ghidoni, PhD,³⁶ Sandro Sorbi, PhD,^{37,38} Martina Bocchetta, PhD,³⁹ Emily Todd, BSc,³⁹ Jens Kuhle, MD ⁴⁰ Christian Barro, MD, PhD,^{40,41} Genetic Frontotemporal dementia Initiative (GENFI),[#] Jonathan D. Rohrer, MD, PhD,³⁹ and Matthis Synofzik, MD ^{1,2}

View this article online at [wileyonlinelibrary.com](https://onlinelibrary.wiley.com/doi/10.1002/ana.26265). DOI: 10.1002/ana.26265

Received Jun 16, 2021, and in revised form Nov 2, 2021. Accepted for publication Nov 3, 2021.

Address correspondence to Dr Matthis Synofzik, Division Translational Genomics of Neurodegenerative Diseases, University of Tübingen, Hoppe-Seyler-Str. 3, 72076 Tübingen, Germany. E-mail: matthis.synofzik@uni-tuebingen.de

[#]Members are listed in Supplement 5.

From the ¹Division Translational Genomics of Neurodegenerative Diseases, Hertie-Institute for Clinical Brain Research and Center of Neurology, University of Tübingen, Tübingen, Germany; ²Center for Neurodegenerative Diseases (DZNE), Tübingen, Germany; ³Department of Neurology, Erasmus Medical Centre, Rotterdam, Netherlands; ⁴Centre for Neurodegenerative Disorders, Department of Clinical and Experimental Sciences, University of Brescia, Brescia, Italy; ⁵Alzheimer's disease and Other Cognitive Disorders Unit, Neurology Service, Hospital Clínic, Institut d'Investigacions Biomèdiques August Pi I Sunyer, University of Barcelona, Barcelona, Spain; ⁶Cognitive Disorders Unit, Department of Neurology, Donostia University Hospital, San Sebastian, Spain; ⁷Neuroscience Area, Biodonostia Health Research Institute, San Sebastian, Spain; ⁸Clinique Interdisciplinaire de Mémoire, Département des Sciences Neurologiques, CHU de Québec, and Faculté de Médecine, Université Laval, Quebec City, Canada; ⁹Center for Alzheimer Research, Division of Neurogeriatrics, Department of Neurobiology, Care Sciences and Society, Bioclinicum, Karolinska Institute, Solna, Sweden; ¹⁰Unit for Hereditary Dementias, Theme Aging, Karolinska University Hospital, Solna, Sweden; ¹¹Fondazione IRCCS Ospedale Policlinico, Milan, Italy; ¹²University of Milan, Centro Dino Ferrari, Milan, Italy; ¹³Department of Clinical Neurosciences, University of Cambridge, Cambridge, UK; ¹⁴Sunnybrook Health Sciences Centre, Sunnybrook Research Institute, University of Toronto, Toronto, Canada; ¹⁵Tanz Centre for Research in Neurodegenerative Diseases, University of Toronto, Toronto, Canada; ¹⁶Department of Clinical Neurological Sciences, University of Western Ontario, London, Canada; ¹⁷Laboratory for Cognitive Neurology, Department of Neurosciences, KU Leuven, Leuven, Belgium; ¹⁸Neurology Service, University Hospitals Leuven, Leuven, Belgium; ¹⁹Leuven Brain Institute, KU Leuven, Leuven, Belgium; ²⁰Faculty of Medicine, University of Lisbon, Lisbon, Portugal; ²¹Fondazione IRCCS Istituto Neurologico Carlo Besta, Milan, Italy; ²²University Hospital of Coimbra (HUC), Neurology Service, Faculty of Medicine, University of Coimbra, Coimbra, Portugal; ²³Center for Neuroscience

Objective: Although the presymptomatic stages of frontotemporal dementia (FTD) provide a unique chance to delay or even prevent neurodegeneration by early intervention, they remain poorly defined. Leveraging a large multicenter cohort of genetic FTD mutation carriers, we provide a biomarker-based stratification and biomarker cascade of the likely most treatment-relevant stage within the presymptomatic phase: the conversion stage. **Methods:** We longitudinally assessed serum levels of neurofilament light (NfL) and phosphorylated neurofilament heavy (pNfH) in the Genetic FTD Initiative (GENFI) cohort ($n = 444$), using single-molecule array technique. Subjects comprised 91 symptomatic and 179 presymptomatic subjects with mutations in the FTD genes *C9orf72*, *GRN*, or *MAPT*, and 174 mutation-negative within-family controls.

Results: In a biomarker cascade, NfL increase preceded the hypothetical clinical onset by 15 years and concurred with brain atrophy onset, whereas pNfH increase started close to clinical onset. The conversion stage was marked by increased NfL, but still normal pNfH levels, while both were increased at the symptomatic stage. Intra-individual change rates were increased for NfL at the conversion stage and for pNfH at the symptomatic stage, highlighting their respective potential as stage-dependent dynamic biomarkers within the biomarker cascade. Increased NfL levels and NfL change rates allowed identification of presymptomatic subjects converting to symptomatic disease and capture of proximity-to-onset. We estimate stage-dependent sample sizes for trials aiming to decrease neurofilament levels or change rates.

Interpretation: Blood NfL and pNfH provide dynamic stage-dependent stratification and, potentially, treatment response biomarkers in presymptomatic FTD, allowing demarcation of the conversion stage. The proposed biomarker cascade might pave the way towards a biomarker-based precision medicine approach to genetic FTD.

ANN NEUROL 2022;91:33–47

Frontotemporal dementia (FTD) is a devastating neurodegenerative disease characterized by progressive decline of executive, behavioral, and language functions,^{1–3} frequently resulting from mutations in the genes *C9orf72*, *GRN*, and *MAPT*.^{4–8} The presymptomatic stages of genetic FTD might provide a unique opportunity to delay or even prevent neurodegeneration by early therapeutic intervention, with promising targeted molecular therapies now entering clinical trials.^{9,10} However, these presymptomatic stages – which encompass the accumulation of progressive molecular and cellular changes in the nervous system before the onset of dementia – remain poorly defined.¹¹ To pave the way for future interventional trials, stratification of the presymptomatic stages based on objective and easily accessible biomarkers is hence urgently needed. This applies particularly to the conversion stage, which immediately precedes the onset of clinically manifest disease and is the likely most treatment-relevant stage in the presymptomatic period.

We here propose blood levels of neurofilament light (NfL) and phosphorylated neurofilament heavy (pNfH) as objective and easily accessible biomarkers for stratifying the presymptomatic period of genetic FTD, providing a

temporal cascade of their biomarker changes. Neurofilaments are neuron-specific cytoskeletal proteins, released upon neuronal damage and, with ultra-sensitive single molecule array (Simoa) assays, reliably quantifiable in peripheral blood.^{12–14} Previous work indicated that NfL blood levels are increased at the symptomatic stage of FTD¹⁵ and also in temporal proximity to the clinical onset of genetic FTD.¹⁶ Similarly, also pNfH blood levels might allow capturing neuronal disintegration and particularly axonal damage, possibly reflecting other features of the neurodegenerative process than NfL.^{12,14} Leveraging a large multicenter cohort of genetic FTD mutation carriers, we here test the hypothesis that – in the biomarker cascade of genetic FTD – the conversion stage is demarcated by increased levels of NfL, but still normal levels of pNfH, whereas the symptomatic stage is marked by increased levels of both neurofilament types.

Methods

Cohort

Subjects were recruited by the Genetic FTD Initiative (GENFI), an international consortium with 25 study sites

and Cell Biology, Faculty of Medicine, University of Coimbra, Coimbra, Portugal; ²⁴Department of Psychiatry, McGill University Health Centre, McGill University, Montreal, Québec, Canada; ²⁵McConnell Brain Imaging Centre, Montreal Neurological Institute, McGill University, Montreal, Québec, Canada; ²⁶Nuffield Department of Clinical Neurosciences, Medical Sciences Division, University of Oxford, Oxford, UK; ²⁷Department of Brain Sciences, Imperial College London, London, UK; ²⁸Division of Neuroscience and Experimental Psychology, Faculty of Medicine, Biology and Health, University of Manchester, Manchester, UK; ²⁹Departments of Geriatric Medicine and Nuclear Medicine, Essen University Hospital, Essen, Germany; ³⁰Neurologische Klinik, Ludwig-Maximilians-Universität München, Munich, Germany; ³¹German Center for Neurodegenerative Diseases (DZNE), Munich, Germany; ³²Munich Cluster of Systems Neurology (SyNergy), Munich, Germany; ³³Department of Neurology, University of Ulm, Ulm, Germany; ³⁴Department of Neurology, Martin-Luther-University Halle-Wittenberg, Halle (Saale), Germany; ³⁵Istituto di Ricovero e Cura a Carattere Scientifico Istituto Centro San Giovanni di Dio Fatebenefratelli, Brescia, Italy; ³⁶Molecular Markers Laboratory, IRCCS Istituto Centro San Giovanni di Dio Fatebenefratelli, Brescia, Italy; ³⁷Department of Neurofarba, University of Florence, Florence, Italy; ³⁸IRCCS Fondazione Don Carlo Gnocchi, Florence, Italy; ³⁹Department of Neurodegenerative Disease, Dementia Research Centre, UCL Institute of Neurology, London, UK; ⁴⁰Neurologic Clinic and Policlinic, MS Center and Research Center for Clinical Neuroimmunology and Neuroscience Basel (RC2NB), University Hospital Basel, University of Basel, Basel, Switzerland; and ⁴¹Department of Neurology, Brigham and Women's Hospital and Harvard Medical School, Boston, MA, USA

Additional supporting information can be found in the online version of this article.

across Europe and Canada. Subjects were patients with FTD caused by mutations in the genes *C9orf72*, *GRN*, or *MAPT* (symptomatic mutation carriers) and their first-degree relatives (ie, either noncarriers serving as controls or presymptomatic mutation carriers).¹⁷ Following the GENFI protocol, subjects underwent comprehensive annual assessments, including neurological and neuropsychological examination, brain imaging, and blood collection, as previously described in detail.¹⁷ For the present study, we included all GENFI subjects with at least one serum sample available ($n = 444$; sample collection = 2015–2019). In total, our study included 444 subjects (thereof 117 *C9orf72*, 104 *GRN*, and 49 *MAPT* carriers, and 174 controls), 196 of whom had longitudinal samples (50 *C9orf72*, 48 *GRN*, and 20 *MAPT* carriers, and 78 controls; see Table 1 for cohort details, stratified by clinical state and gene).

Our study cohort comprises a subset of subjects (41%) also included in a previous GENFI study¹⁶ ($n = 184$, hereof 79 presymptomatic, 31 symptomatic, and 4 converting carriers, and 70 controls). Accordingly, blood samples from 388 (52%) of the 748 study visits from which blood samples were assessed in our study were also included in this previous study, but now independently measured.

Local ethics committees at each site approved the study. All subjects provided written informed consent prior to participation according to the Declaration of Helsinki.

Mutation carriers were considered symptomatic if fulfilling established diagnostic criteria for FTD, including behavioral variant FTD and primary progressive aphasia phenotypes.^{1,2} *C9orf72* mutation carriers were also considered symptomatic if fulfilling established criteria for amyotrophic lateral sclerosis (ALS),¹⁸ but not FTD. Those mutation carriers who were presymptomatic at baseline but became symptomatic during follow-up are referred to as converters (6 *C9orf72* and 1 *GRN* carriers). Disease severity was assessed with the Clinical Dementia Rating scale plus FTLT modules (CDR plus NACC FTLT), using the global score.¹⁹ As the symptomatic stage can alternatively also be defined by mutation carriers having a CDR plus NACC FTLT score ≥ 1 , we also ran the main analyses with this criterion. Clinical raters were blinded to the genetic status of at-risk individuals unless these had undergone predictive testing.

Neurofilament quantification

Blood samples were centrifuged (2,000 g, 10 minutes, at room temperature). Serum was frozen at -80°C within 3 hours after collection, shipped and analyzed without any previous thaw–freeze cycle. We measured neurofilament

levels in duplicates by single molecule array (Simoa) technique on the Simoa HD-1 Analyzer (Quanterix, Lexington, MA, USA), using the NF-light Advantage kit for NfL¹³ and the pNF-heavy Discovery kit (Quanterix) for pNfH quantification,¹⁴ according to the manufacturer's instructions (dilution: 1/4). For NfL, all measurements had a coefficient of variation (CV) below 20%. For pNfH, measurements with CV values above 20% ($n = 21$) were excluded to ensure comparable quality. For both analytes, concentrations were in the previously established range of quantification.^{13,14} Both NfL and pNfH showed high technical and intraindividual biological stability (Tables 2 and 3, Fig 5). Technicians were blinded to the genotypic and clinical status of the samples. Longitudinal samples were measured in the same batch.

Volumetric brain imaging

For quantification of global and frontal brain atrophy, whole-brain grey matter volume and regional volumes were quantified by semi-automated segmentation methods, based on T1-weighted volumetric magnetic resonance imaging (MRI) scans, and grey matter volumes were expressed as percentages of total intracranial volume, as previously described.¹⁷

Statistical analysis

Baseline levels of neurofilaments. We used Mann–Whitney U tests (2-sided, significance level: $p < 0.05$, Bonferroni-corrected within each biomarker) to compare neurofilament baseline levels among clinical states (ie, presymptomatic carriers, converters, symptomatic carriers, and controls) and among groups of different disease severity in the early disease stages (unaffected carriers: CDR plus NACC FTLT = 0, mildly affected carriers: CDR plus NACC FTLT = 0.5, definitely affected carriers: CDR plus NACC FTLT ≥ 1 , and controls). To correct the group effects for the age-related Nf increase observed in controls,^{15,20} we calculated the z-score of each subject in relation to the neurofilament distribution in controls at the same age.²¹ For this, the difference between the measured level and the level predicted for controls at the same age was standardized relative to the distribution in controls at this age. Levels in controls were modeled by linear regression on the level of log-transformed data. Wherever possible, we report the effect size r for the applied test.

Annualized change rates of neurofilaments. To capture the temporal dynamics of neurofilament levels within each subject, we calculated the individual annualized change rate (for all subjects for whom longitudinal neurofilament measurements were available, $n = 196$) as the regression coefficient of individual linear regressions of the neurofilament

TABLE 1. Cohort Characteristics at Baseline

Group	Subjects	Subjects with longitudinal samples	Follow-up duration (years)	Male sex	Age (years)	MMSE	CDR plus NACC FTLD	Disease onset (years)	Disease duration (years)
presymptomatic	172	74	1.42 (1.03–2.47)	37%	41.2 (33.2–50.5)	30 (29–30)	0 (0–0)		
- C9orf72	64	25	2.15 (1.30–2.87)	36%	42.5 (33.7–52)	30 (29–30)	0 (0–0)		
- GRN	74	35	1.10 (1.01–2.27)	39%	41.2 (33.8–50.7)	30 (30–30)	0 (0–0)		
- MAPT	34	14	1.98 (1.12–2.16)	35%	36 (31.9–45.9)	30 (30–30)	0 (0–0)		
Converter	7	6	1.68 (1.11–2.45)	71%	62.5 (52.2–65.6)	30 (29–30)	0 (0–0)		
- C9orf72	6	5	2.08 (1.28–2.57)	67%	57.9 (51.7–63.5)	30 (30–30)	0 (0–0)		
- GRN	1	1	1.03	100%	67.8	28	0		
Symptomatic	91	38	1.13 (0.99–1.77)	58%	63.3 (57.6–68.4)	25 (19–27)	2 (1–3)	57 (53–63)	4.4 (2.5–6.4)
- C9orf72	47	20	1.22 (1.00–1.91)	66%	64.6 (57.5–70.2)	26 (23–28)	2 (1–3)	57 (53–63)	5.4 (3–7.2)
- GRN	29	12	1.02 (0.97–1.08)	48%	63.4 (59–68.1)	22 (14–26)	2 (1–3)	60 (55–65)	2.7 (1.9–4.9)
- MAPT	15	6	2.04 (1.76–2.19)	53%	62.5 (55.7–65.1)	24 (19–28)	2 (2–3)	54 (46–59)	6.0 (3.3–8.5)
Non-carriers	174	78	1.18 (1.02–2.23)	43%	44.1 (36.6–55.2)	30 (29–30)	0 (0–0)		

The clinical phenotype of symptomatic mutation carriers was behavioral variant FTD (n = 60), primary progressive aphasia (n = 16), amyotrophic lateral sclerosis (n = 7), frontotemporal dementia with amyotrophic lateral sclerosis (n = 3), corticobasal syndrome (n = 2), progressive supranuclear palsy (n = 1), and dementia not otherwise specified (n = 2). For converters, the age at conversion was 65.7 (54.7–67.4) years. The global follow-up duration across all subjects with longitudinal samples was 1.19 (1.02–2.23) years. Data are reported as median and interquartile range. CDR plus NACC FTLD = Clinical Dementia Rating scale plus FTLD modules; MMSE = Mini-Mental State Examination.

level over age. The annualized change rates were compared between clinical states with Mann–Whitney *U* tests (as specified above).

Linear mixed-effects models. To characterize the disease stages of genetic FTD in terms of both neurofilament levels and their change rates, we used linear mixed-effects models of longitudinal neurofilament data, thus considering the covariance between repeated measurements of each subject.^{16,22} In the models, we included clinical status (presymptomatic stage, conversion stage, symptomatic stage, and controls as the reference group), age (centered at the mean baseline age of all subjects), and time from baseline (ie, the first serum sample) as fixed effects, the interaction of clinical status and time from baseline, and the random variable subject, modeled by random intercepts (R packages: *lme4* and *effects*). The addition of random slopes did not improve the model fit. Neurofilament levels were log-transformed to meet the models' assumptions.

Biomarker cascade model. To assess the dynamics of biomarker changes in terms of timing and effect size uniformly across several biomarkers, we modeled the normalized baseline biomarker values (as z-score) over

age with polynomials and compared the predicted values of carriers with those of controls at the same age (as z-score difference).^{23,24} For each biomarker, the biomarker values (log-transformed for both NfL and pNfH) were normalized relative to their distribution in controls (ie, transformed to z-scores). The z-scores were modeled with orthogonal polynomials over age, separately for carriers and controls to allow different dynamics between groups. Higher-order polynomial terms were included if significant (max. cubic terms). The model predictions for carriers were compared to the predictions for controls at the same age by calculating the z-score difference. We applied this approach to all mutation carriers together and, additionally, to the three genetic groups separately, allowing exploration also of gene-specific biomarker cascades.

Sample size estimation for intervention trials. We estimated stage-dependent sample sizes for future treatment trials using the reduction of neurofilament levels towards the levels observed in healthy controls as outcome measure.^{21,25} We estimated the total sample size required to detect a given control-adjusted relative reduction of neurofilament levels (20–80%) in the treatment arm, assuming that null mean change over

TABLE 2. Within- and Between-run Precision of the NfL and pNfH Assay

Analyte	Mean concentration (pg/ml)	Within-run precision (%)	Between-run precision (%)
NfL	6.2	7.5	9.7
NfL	19.0	3.3	3.6
NfL	36.6	7.1	6.0
pNfH	84.4	3.6	5.5
pNfH	23.9	6.2	13.5
pNfH	235.5	4.0	6.1

Within-run precision and between-run precision⁴⁴ were derived from 4 consecutive runs of the same biological sample, using 3 samples with different analyte concentrations.
NfL = neurofilament light; pNfH = phosphorylated neurofilament heavy.

time occurred in the placebo arm of the trial. We based the assumed intersubject variability in the hypothetical trial on the measured intrasubject variability in the change of analyte levels (from baseline to first follow-up) in our mutation carriers. The estimation further assumed equal numbers of subjects in both study arms (ie, allocation ratio 1:1), $\alpha = 0.05$, $\beta = 0.05$, 2-tailed independent t tests, and the use of log-transformed biomarker levels. It was performed with GPower version 3.1 software (Kiel, Germany). We also explored the sample size which would be required for trials aiming to normalize the increased annualized change rates of NfL during the conversion stage (instead of reducing its absolute levels), using the standardized response mean in analogy to approaches in other neurodegenerative diseases.²⁶

Data availability

The de-identified data of this article can be accessed on reasonable request addressed to the GENFI consortium.

Results

NfL and pNfH levels are increased at the symptomatic, but not the presymptomatic stage

Baseline levels of serum NfL in symptomatic carriers (38.7 pg/ml [23.7–60.0]) were significantly higher than in controls (6.6 pg/ml [4.8–9.6]; $p < 0.001$, effect size: $r = 0.74$; Fig 1A and B). NfL levels in symptomatic carriers were significantly increased also in comparison to presymptomatic carriers (6.8 pg/ml [4.8–9.0], $p < 0.001$, $r = 0.76$), whereas NfL levels of presymptomatic carriers did not differ significantly from those of controls (not significant [ns.], $r = 0.01$). Similarly, also baseline levels of serum pNfH were significantly higher in symptomatic carriers (156.0 pg/ml [82.9–399.0]) than in both controls (47.6 pg/ml [23.7–105.6], $p < 0.001$, $r = 0.47$) and presymptomatic carriers (40.7 pg/ml [20.1–93.2], $p < 0.001$, $r = 0.51$), whereas pNfH levels of presymptomatic carriers did not differ significantly from those of controls (ns., $r = 0.06$; Fig 1C and D). The increase of neurofilament levels from the presymptomatic to the symptomatic stage was quantitatively more pronounced for NfL than for pNfH, as evidenced by its respective effect sizes (NfL: $r = 0.76$, and pNfH: $r = 0.51$). The results were confirmed if corrected for the age-related neurofilament increase observed in controls (NfL: symptomatic vs. controls: $p < 0.001$, $r = 0.68$, symptomatic vs. presymptomatic: $p < 0.001$, $r = 0.65$, presymptomatic vs. controls: ns., $r = 0.10$; pNfH: symptomatic vs. controls: $p < 0.001$, $r = 0.28$, symptomatic vs. presymptomatic: $p < 0.001$, $r = 0.29$, presymptomatic vs. controls: ns., $r = 0.02$). Moreover, the increases of NfL and pNfH levels from the presymptomatic to the symptomatic stage were both confirmed within each of the three genetic subgroups (Fig 1E and F).

TABLE 3. Intra-individual Stability of NfL and pNfH Levels in Mutation Carriers and Controls

Subject group	NfL	pNfH	Sampling interval (years)
Overall	0.947 (0.930–0.960)	0.947 (0.930–0.961)	1.07 (1.00–1.19)
Controls	0.845 (0.768–0.899)	0.940 (0.906–0.962)	1.07 (1.00–1.19)
Presymptomatic carriers	0.834 (0.749–0.892)	0.943 (0.909–0.964)	1.09 (1.01–1.21)
Symptomatic carriers	0.922 (0.857–0.959)	0.903 (0.814–0.950)	1.05 (0.98–1.14)

We assessed the intra-individual stability of neurofilament levels by calculating the intraclass correlation coefficient (ICC) of each analyte (model: 2-way mixed, single measures, absolute agreement, implemented in the R package *irr*), using the longitudinal neurofilament data (log-transformed) of subjects' baseline and first follow-up visit (74 presymptomatic, 38 symptomatic, and 78 control subjects). The table reports the ICC estimates with 95% confidence intervals and the sampling interval (median and IQR).

IQR = interquartile range; NfL = neurofilament light; pNfH = phosphorylated neurofilament heavy.

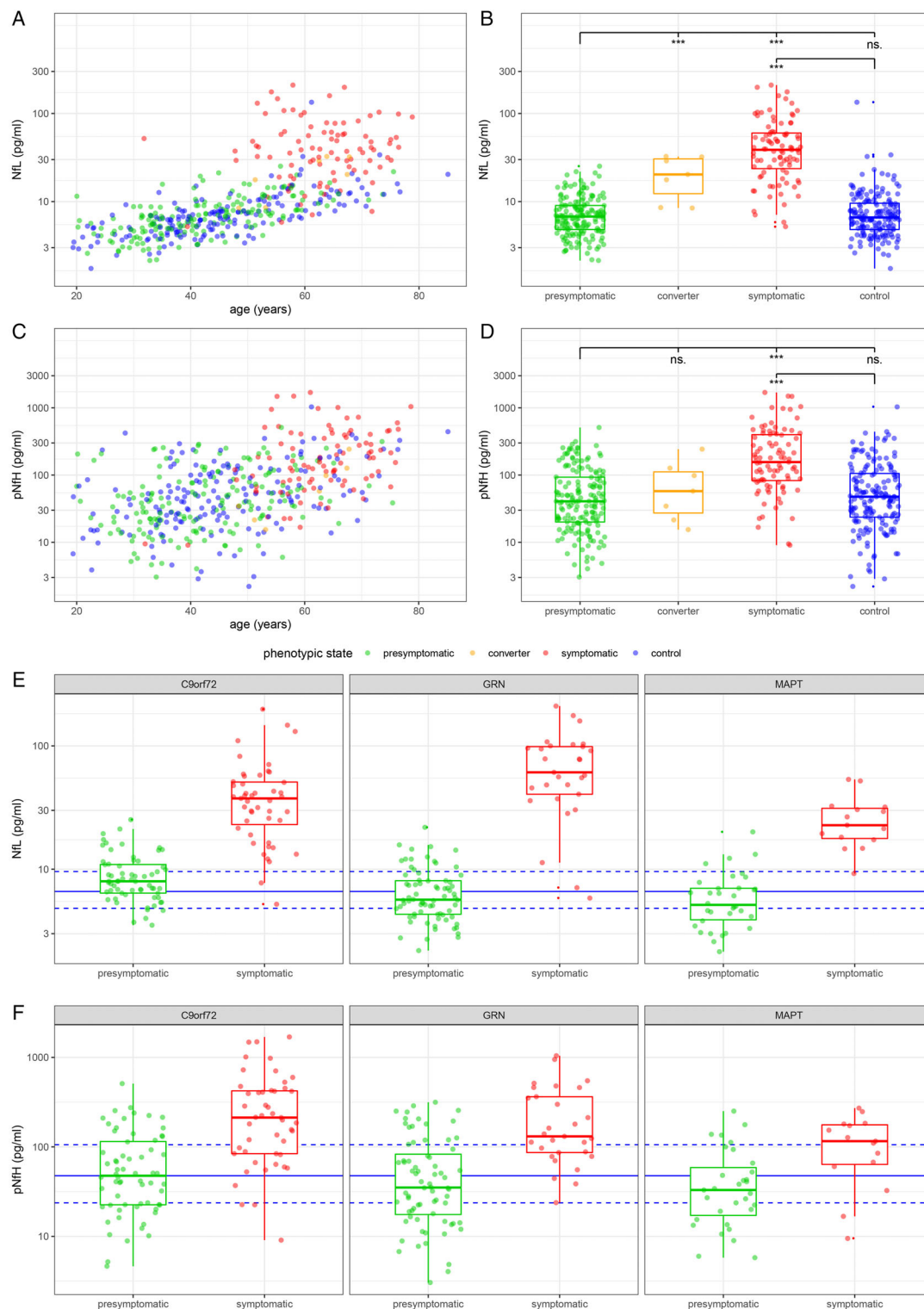


FIGURE 1: NfL and pNfH levels at the presymptomatic, conversion, and symptomatic stage of genetic FTD. Serum levels of NfL (A, B) and pNfH (C, D) were measured in FTD mutation carriers at the presymptomatic (*green*), conversion (*orange*), and symptomatic disease stage (*red*), and in mutation-negative controls (*blue*). For masking purposes, a jitter was added to subjects' age (A, C), whereas analyses were done on raw data. Boxes visualize median, lower, and upper quartiles, whiskers extend to data within 1.5-IQR of the median, and dots represent individual values. Stages were compared with Mann–Whitney *U* tests (** $p < .001$, ns $p \geq .05$, two-tailed, Bonferroni-corrected). For each of the three genetic subgroups (E), baseline NfL levels were significantly higher in symptomatic than presymptomatic carriers (*C9orf72*: $p < 0.001$, $r = 0.76$, *GRN*: $p < 0.001$, $r = 0.72$, *MAPT*: $p < 0.001$, $r = 0.76$). For reference, baseline levels of controls are indicated by blue horizontal lines (median with IQR). In addition, baseline pNfH levels were significantly higher in symptomatic than presymptomatic carriers for each of the three subgroups (F) (*C9orf72*: $p < 0.001$, $r = 0.53$, *GRN*: $p < 0.001$, $r = 0.51$, *MAPT*: $p = 0.009$, $r = 0.43$, post hoc tests corrected for multiple comparisons). IQR = interquartile range; NfL = neurofilament light; pNfH = phosphorylated neurofilament heavy.

NfL levels are increased at the conversion stage, whereas pNfH levels are still normal

Those presymptomatic mutation carriers who developed symptomatic disease during the longitudinal follow-up (termed converters) showed significantly higher baseline levels of NfL (20.3 pg/ml [13.1–30.6]) than non-converting presymptomatic carriers (6.8 pg/ml [4.8–9.0], $p < 0.001$, $r = 0.27$; see Fig 1A and B), indicating that the NfL increase in genetic FTD precedes the transition from the presymptomatic to the symptomatic disease stage. NfL levels hereby accurately distinguished converters from non-converting presymptomatic carriers (area under the curve [AUC] = 0.91 [0.80–1.00], estimate and 95% confidence interval), indicating that NfL levels allow predicting future conversion. In contrast, baseline levels of pNfH were not significantly higher in converters (57.7 pg/ml [28.0–112.5]) than in presymptomatic carriers (40.7 pg/ml [20.1–93.2], ns., $r = 0.06$; see Fig 1C and D). Each of these findings was confirmed if corrected for age-related neurofilament increases (NfL: converters vs. presymptomatic: $p = 0.009$, $r = 0.21$, pNfH: converters vs. presymptomatic: ns., $r = 0.05$). Thus,

the conversion stage was marked by increased NfL levels in combination with still normal pNfH levels.

Individual change rates of neurofilament levels are increased at the conversion stage for NfL, and at the symptomatic stage for pNfH

In the group of converters, we observed an intra-individual longitudinal increase of NfL levels with proximity to the onset of the symptomatic disease stage (Fig 2A). Accordingly, the annualized change rate of NfL levels was significantly higher in converters (7.20 pg/[ml·year], 4.70–10.19) than in presymptomatic carriers (0.25 pg/[ml·year], [−0.27–0.87]; $p < 0.001$, $r = 0.40$), indicating an intra-individual increase of NfL levels in subjects during the conversion stage (see Fig 2B). The annualized change rate of NfL levels did not differ significantly between presymptomatic carriers and controls (0.13 pg/[ml·year], [−0.66–0.65], ns., $r = 0.10$), nor between presymptomatic and symptomatic carriers (1.18 pg/[ml·year], [−1.88–13.20], ns., $r = 0.12$), suggesting that intra-individual NfL levels might be stable at normal levels at the presymptomatic stage and, after the

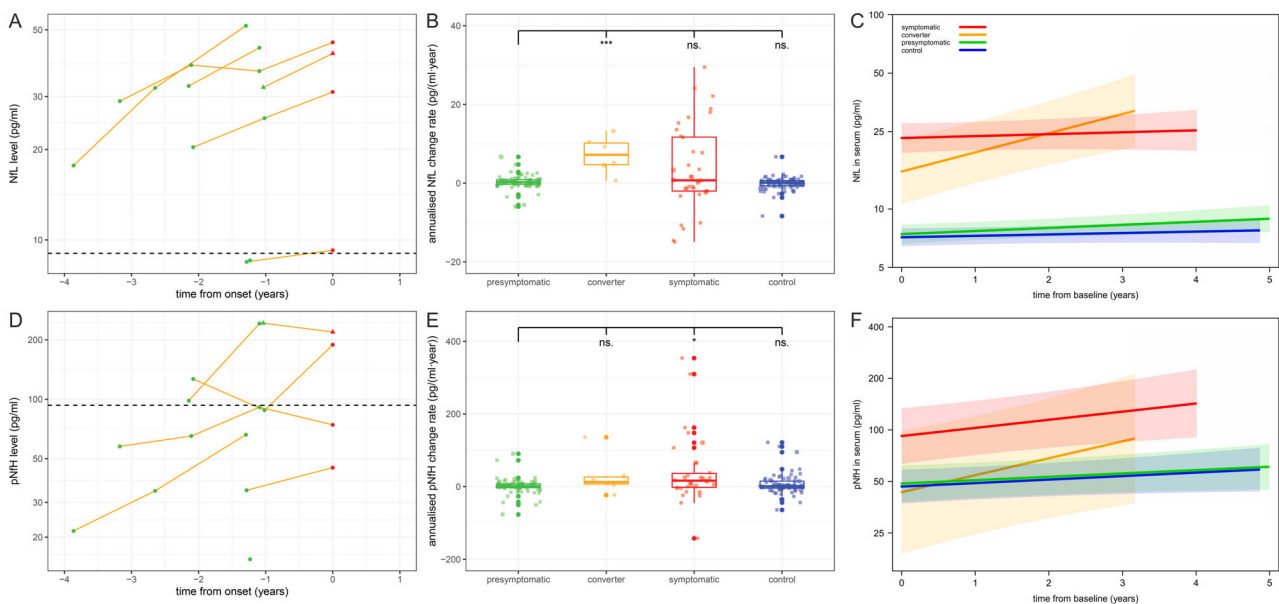


FIGURE 2: Individual longitudinal trajectories and stage-dependent longitudinal dynamics of NfL and pNfH levels in genetic FTD. For mutation carriers converting from the presymptomatic to the symptomatic stage (converters), the individual longitudinal trajectories of NfL (A) and pNfH levels (D) are plotted over the time from the clinically observed disease onset, with negative time values corresponding to the presymptomatic stage. The dashed line marks the upper quartile of baseline neurofilament levels in non-converting presymptomatic mutation carriers. The individual annualized change rates of NfL (B) and pNfH levels (E) were estimated by individual linear regressions for mutation carriers at the presymptomatic (green), conversion (orange), and symptomatic stage (red), and for controls (blue). Boxes visualize median, lower, and upper quartiles, whiskers extend to data within 1.5-IQR of the median, and dots represent individual values. For improved readability, two extreme outliers of the pNfH change rate at the symptomatic stage (−586 pg/[ml·year], +662 pg/[ml·year]) are not displayed. Stages were compared with Mann–Whitney U tests (***) $p < .001$, * $p < .05$, ns $p \geq .05$, two-tailed, Bonferroni-corrected). We modeled the longitudinal neurofilament levels for NfL (C) and pNfH (F) in relation to time from baseline, clinical state (ie, presymptomatic carrier, converter, symptomatic carrier, and control) and age at baseline, using linear mixed-effects models. The figures display the model predictions at mean baseline age, with shaded areas representing 95% confidence intervals. IQR = interquartile range; NfL = neurofilament light; pNfH = phosphorylated neurofilament heavy.

conversion stage, stable at increased levels at the symptomatic stage (see Fig 2B). NfL change rates accurately distinguished converters from non-converting carriers (AUC = 0.94 [0.83–1.00]). For pNfH, the change rate was significantly higher in symptomatic carriers (16.40 pg/[ml·year], -3.86 – 58.40) than in presymptomatic carriers (1.28 pg/[ml·year], $[-2.93$ – $7.52]$, $p = 0.018$, $r = 0.27$; see Fig 2D and E), but did not differ significantly between presymptomatic subjects and converters (12.83 pg/[ml·year], $[7.35$ – $26.34]$, ns., $r = 0.23$), nor between presymptomatic subjects and controls (0.83 pg/[ml·year], $[-4.25$ – $15.06]$, ns., $r = 0.05$), suggesting that pNfH levels might remain stable during the

presymptomatic and conversion stage, but – unlike NfL levels – increase at the symptomatic stage.

Modeling the disease stages of genetic FTD in terms of NfL and pNfH levels and their change rates

To comprehensively characterize the disease stages in terms of both neurofilament levels and their change rates, a linear mixed-effects model was calculated, allowing to integrate all longitudinal follow-up neurofilament measurements and intraindividual changes as well as to correct for baseline age. The variable time from baseline hereby allowed estimation of a regression

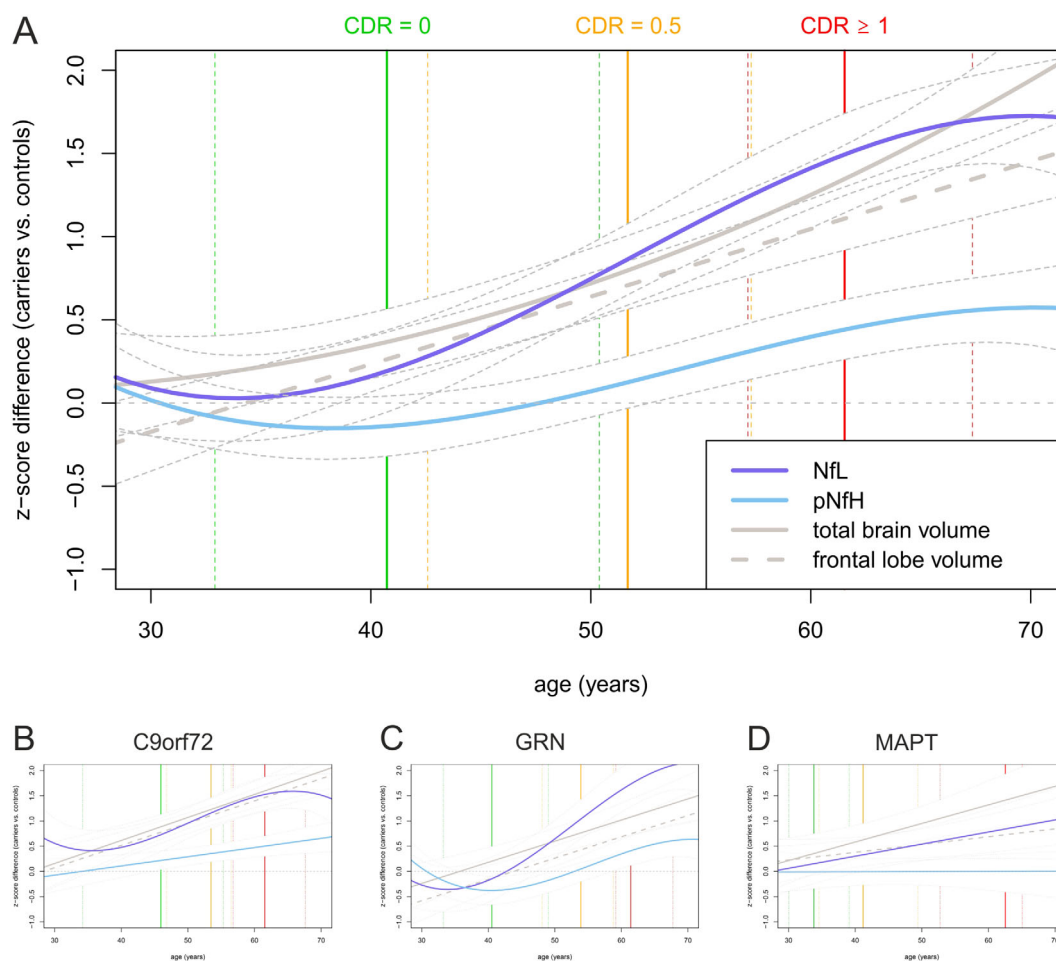


FIGURE 3: Biomarker cascade of NfL, pNfH, and volumetric MRI changes across the early CDR stages of genetic FTD. (A) To assess the relative timing and effect size of biomarker changes uniformly for each biomarker (NfL, pNfH, global brain volume, and frontal brain volume), we modeled the normalized biomarker values as polynomial functions of subjects' age and compared the model predictions for carriers to the model predictions for controls at the same age, calculating the z-score difference. Increases of the z-score difference towards positive values indicate that the biomarker values become more pathological in the mutation carrier group (ie, increases of neurofilament levels and decreases of brain volumes), whereas a z-score difference of zero indicates that the respective biomarker values do not differ between mutation carriers and controls. For each biomarker, the confidence interval is displayed by dotted lines. The colored vertical lines indicate the baseline age (median and IQR) of mutation carriers grouped by disease severity (unaffected carriers: CDR plus NACC FTLD = 0, mildly affected carriers: CDR plus NACC FTLD = 0.5, and definitely affected carriers CDR plus NACC FTLD ≥ 1), as observed in the present cohort. (B–D) The same modeling approach was analogously applied to the three genetic groups of mutation carriers (B: *C9orf72*, C: *GRN*, and D: *MAPT*) to explore gene-specific dynamics and effect sizes of the biomarker cascade. CDR = Clinical Dementia Rating; FTD = frontotemporal dementia; IQR = interquartile range; MRI = magnetic resonance imaging; NfL = neurofilament light; pNfH = phosphorylated neurofilament heavy.

coefficient reflecting the biomarker annual change rate, whereas its interaction with the variable clinical state allowed capturing differences in the annual change rates between clinical states. The model showed a significant effect of subjects' clinical status on NfL levels ($p < 0.001$) and a significant interaction of time from baseline with clinical status ($p = 0.008$; see Fig 2C; Supplement 1 for complete statistical results). Compared with controls, NfL levels were significantly increased in converters ($p < 0.001$) and symptomatic carriers ($p < 0.001$), but not in presymptomatic carriers ($p = 0.631$). The annual change rate of NfL levels was significantly increased in converters ($p < 0.001$), but neither in presymptomatic ($p = 0.377$) nor symptomatic carriers ($p = 0.854$), indicating that the increase of NfL levels occurs at the conversion stage. For pNfH, the model showed a significant effect of clinical status on pNfH levels ($p = 0.021$), without significant interaction of time from baseline with clinical status (Fig 2F; Supplement 2). Compared with controls, pNfH levels were significantly increased in symptomatic carriers ($p = 0.003$),

but not in presymptomatic carriers ($p = 0.808$) or converters ($p = 0.865$), indicating that the pNfH increase is linked to the symptomatic stage. Thus, the analysis by linear mixed-effects models further supports the notion that the combined temporal dynamics of both neurofilament types might allow demarcating the conversion stage: its onset is marked by increased NfL levels and NfL change rates (but still normal pNfH levels), whereas its completion with transition to the symptomatic stage is marked by increased pNfH levels.

Modeling the multimodal biomarker cascade of genetic FTD: NfL increase concurs with brain atrophy onset, while pNfH increase starts close to clinical onset – with varying temporal dynamics and effect sizes in the three genetic FTD groups

To further assess the temporal dynamics of each biomarker (NfL, pNfH, global and frontal brain volume), we

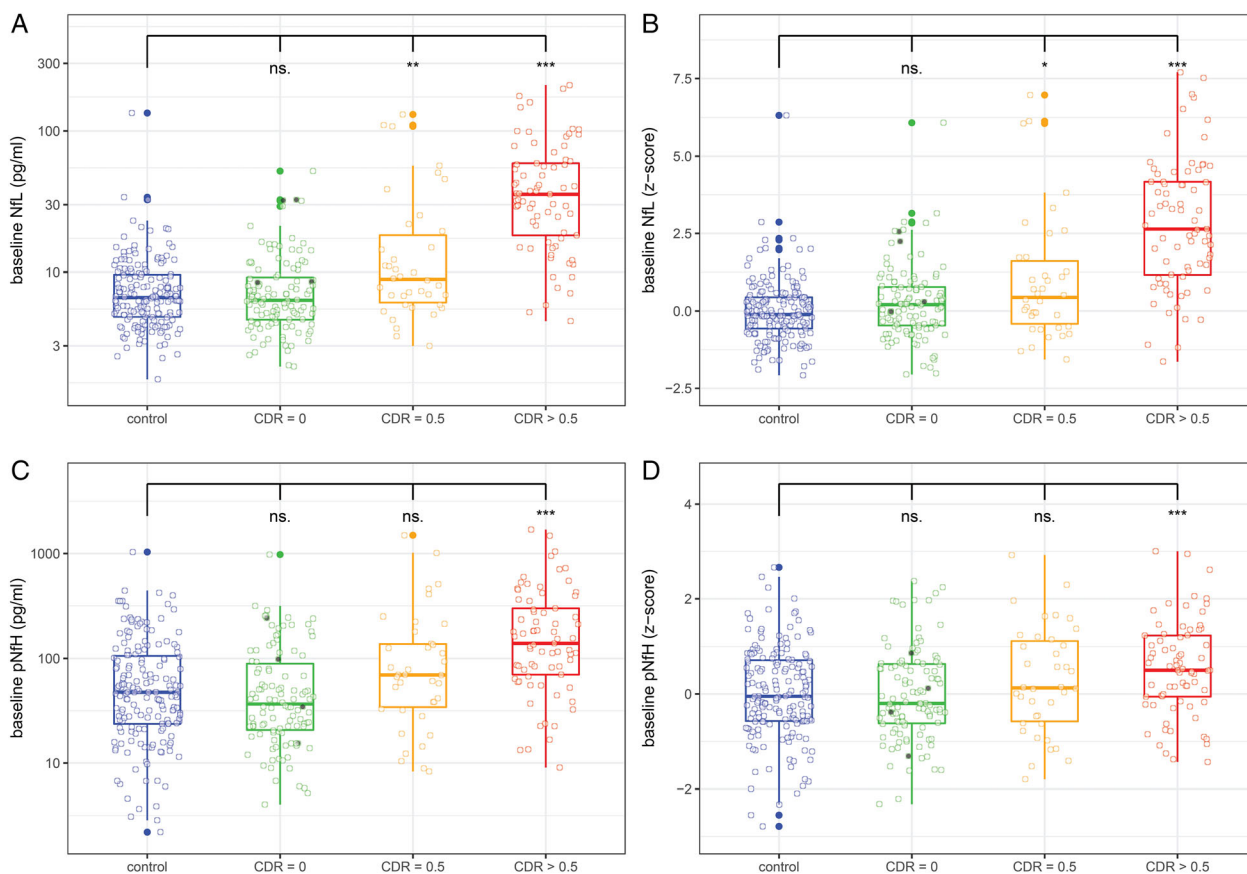


FIGURE 4: Stratification of the early stages of disease severity in genetic FTD by NfL and pNfH levels. Baseline levels of NfL (A) and pNfH (C) were compared between unaffected carriers (CDR plus NACC FTLD = 0), mildly affected carriers (CDR plus NACC FTLD = 0.5), definitely affected carriers (CDR plus NACC FTLD ≥ 1) and controls. To take into consideration the age-related increase of neurofilament levels, the absolute levels (A, C) were corrected for the age-related increase observed in controls by z-transformation (B, D). Boxes visualize median, lower, and upper quartiles, whiskers extend to data within 1.5-IQR of the median, and circles represent individual values. Baseline values of converters are marked by circles filled with grey. Groups were compared with Mann-Whitney U tests (***) $p < .001$, ** $p < .01$, * $p < .05$, ns $p \geq .05$, 2-tailed, Bonferroni-corrected). CDR = Clinical Dementia Rating; FTD = frontotemporal dementia; IQR = interquartile range; NfL = neurofilament light; ns. = not significant; pNfH = phosphorylated neurofilament heavy. [Color figure can be viewed at www.annalsofneurology.org]

used polynomials to model the normalized biomarker values (z-scores) over age and compared the predicted biomarker values of mutation carriers to those of controls at the same age (Fig 3A). The z-score difference allowed capturing timing and effect size of biomarker changes uniformly across all biomarkers. In this biomarker cascade,

the NfL z-score difference started to increase at age 42 years (as indicated by the time at which the 95% confidence interval of the z-score difference ceases to overlap zero), thus preceding the observed clinical onset at age 57 years (53–63 years) by approximately 15 years. In contrast, the pNfH z-score difference started to increase at age

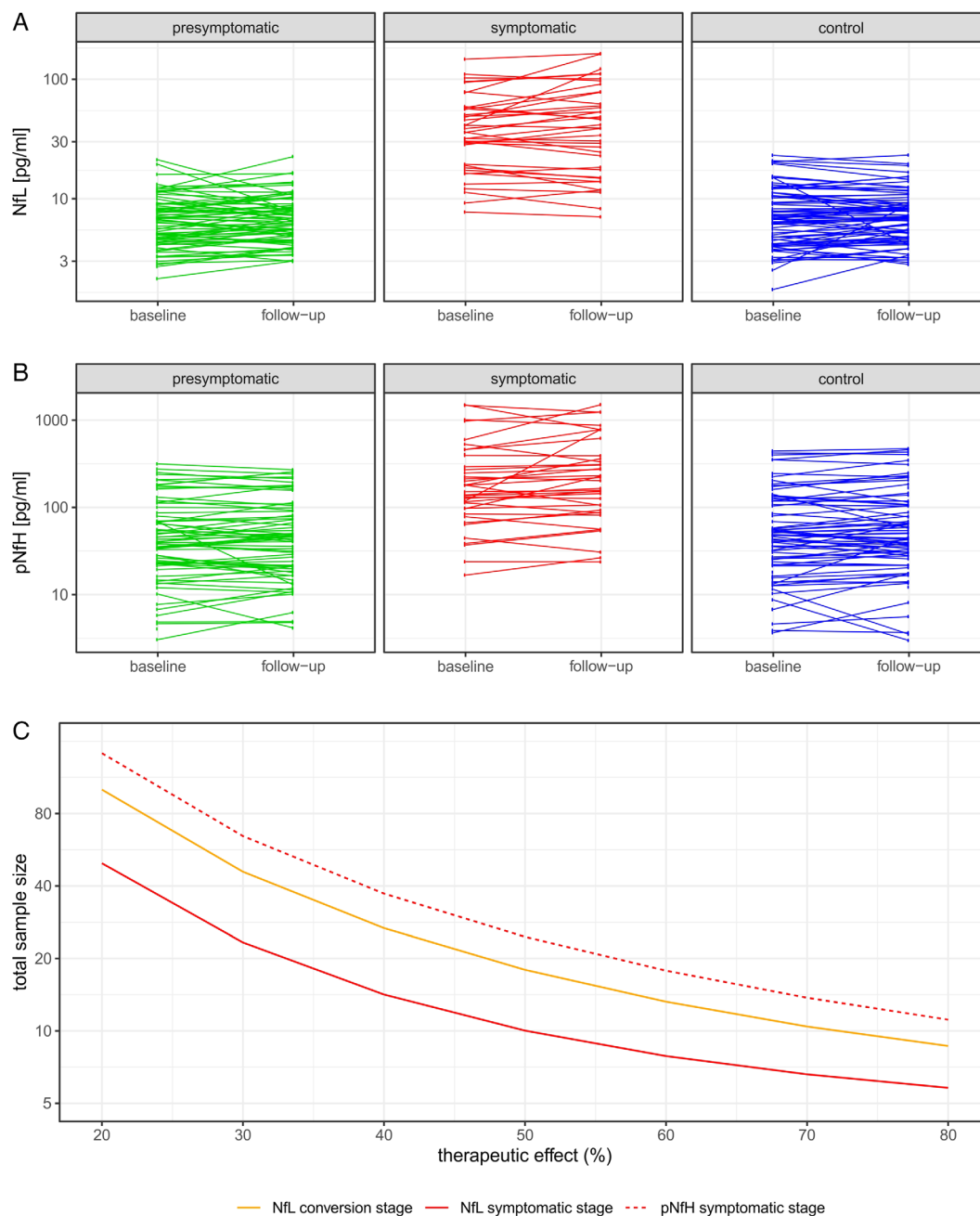


FIGURE 5: Within-subject stability of neurofilament levels and stage-dependent sample size estimates for intervention trials in genetic FT. The intra-individual stability of NfL (A) and pNfH (B) serum levels from baseline to first follow-up was assessed in presymptomatic and symptomatic carriers and control subjects. Lines link data of the same individuals. Sample size estimations (C) were performed for hypothetical intervention trials using the reduction of neurofilament levels as outcome measure, taking into consideration the disease stage. The estimated total sample size (ie, sum of subjects in both study arms) is plotted over the assumed therapeutic effect for lowering the neurofilament level in mutation carriers towards the levels observed in healthy controls. FT = frontotemporal dementia; NfL = neurofilament light; pNfH = phosphorylated neurofilament heavy. [Color figure can be viewed at www.annalsofneurology.org]

53 years, close to the observed clinical onset. For both NfL and pNfH, the z-score difference reached a plateau at the late symptomatic stage. Analogous analysis showed that volumetric changes of the global brain volume and the frontal lobe volume started at age 39 years, thus preceding the observed onset by approximately 18 years. In summary, the NfL increase in mutation carriers preceded clinical disease onset and concurred with brain atrophy onset, whereas the pNfH increase started close to clinical onset (see Fig 3A). Exploratory analogous modeling in the 3 genetic subgroups of mutation carriers (see Fig 3B–D) suggested that, in each the *C9orf72* and *GRN* group, an NfL increase started at the presymptomatic stage (reaching a pronounced z-score level of abnormality, with NfL effect sizes in the *GRN* group larger than those of the MRI measures), followed by a pNfH increase with the onset of the symptomatic stage (reaching a less pronounced z-score level of abnormality). In the *MAPT* group, the NfL increase (also starting at the presymptomatic stage) was, however, slower and the pNfH increase appeared absent. The MRI measures yielded stronger effect sizes than the NfL increase in the *MAPT* group (see Fig 3D).

The combination of NfL and pNfH levels allows stratification of FTD disease severity in the early disease stages

NfL levels were significantly increased in both mildly affected carriers (CDR plus NACC FTLD = 0.5 at baseline visit, $p = 0.004$, $r = 0.21$) and definitely affected carriers (CDR plus NACC FTLD ≥ 1 , $p < 0.001$, $r = 0.68$), each compared with controls, whereas unaffected carriers (CDR plus NACC FTLD = 0) did not show increased NfL levels (ns., $r = 0.03$; Fig 4A). This finding was confirmed if NfL levels were corrected for the age-related increase observed in controls. The age-corrected NfL z-scores were significantly increased in both mildly affected carriers ($p = 0.017$, $r = 0.19$) and definitely affected carriers ($p < 0.001$, $r = 0.62$), but not in unaffected carriers (ns., $r = 0.11$; see Fig 4B). In contrast, pNfH levels were increased in definitely affected carriers ($p < 0.001$, $r = 0.40$), but not in unaffected (ns., $r = 0.08$) or mildly affected carriers (ns., $r = 0.13$; see Fig 4C). Likewise, age-corrected pNfH z-scores were significantly increased in definitely affected carriers ($p < 0.001$, $r = 0.23$), but not in unaffected (ns., $r = 0.03$) or mildly affected carriers (ns., $r = 0.08$; see Fig 4D). Thus, already first mild clinical manifestations were captured by the NfL increase, whereas the definite clinical manifestation of FTD was reflected by the combined increase of both NfL and pNfH.

Add-on analysis suggested that neurofilament levels in genetic FTD might also correlate with the extent of

motoneuron involvement, with differential capture of upper versus lower motoneuron involvement by NfL and pNfH (Supplement 3).

Both NfL and pNfH show high technical and intra-individual biological stability

Technical stability was comparable for NfL and pNfH, as demonstrated by similarly high within- and between-run precision (see Table 2). Moreover, biological stability (ie, intraindividual analyte stability) was comparable for NfL and pNfH, as evidenced by high intraclass correlation coefficients of both analytes in longitudinal measurements (see Table 3, Fig 5A and B).

Neurofilament levels as disease-stage-dependent outcome parameters for intervention trials

We estimated sample sizes for intervention trials using the reduction of neurofilament levels as outcome parameter, taking into consideration the respective disease stage of genetic FTD. Our estimates indicate that, to detect a therapeutic effect size of 50% if using NfL levels, the required total sample size would be 12 subjects at the symptomatic stage (for 1:1 randomization, see Fig 5C for visualization of a range of other possible therapeutic effect sizes) and 18 subjects at the conversion stage. For a more modest effect size of 30%, 24 subjects at the symptomatic stage (32 subjects for 3:1 randomization) and 46 subjects at the conversion stage would be needed. If using pNfH levels as outcome parameters at the symptomatic stage, 26 subjects would be needed for an effect size of 50% and 66 subjects for an effect size of 30%. For intervention trials aiming to normalize the increased annualized change rates of NfL during the conversion stage (instead of reducing its absolute levels), our estimates indicate that 88 subjects would be required.

Discussion

Stratification of the presymptomatic phase of genetic FTD via objective and easily accessible molecular biomarkers is warranted to pave the way for upcoming targeted treatment trials. Leveraging the longitudinal multicenter GENFI cohort, we here demonstrate a cascade of biomarker changes in presymptomatic genetic FTD, where the NfL increase in blood precedes the hypothetical clinical onset by 15 years, here concurring with the onset of global brain atrophy, followed by a pNfH increase starting close to clinical onset. Moreover, we demonstrate that neurofilament levels allow demarcating the conversion stage, for which the onset is marked by increased levels and intra-individual change rates of NfL (but still normal pNfH levels), and its completion with transition to the

symptomatic stage by increased pNfH levels. Thus, NfL and pNfH levels might provide disease stage-dependent stratification biomarkers and, possibly, treatment outcome biomarkers in genetic FTD.

Our study suggests an association of the onset of the NfL increase to the conversion stage, given that both NfL levels and NfL increase rates were increased in presymptomatic carriers converting to symptomatic disease, but not in carriers remaining presymptomatic during longitudinal follow-up. The NfL increase preceded the mean clinical onset observed in the symptomatic subjects of our cohort by 15 years, thus even earlier than estimated in previous studies.¹⁶ Moreover, as the NfL increase concurred with the onset of both global and frontal brain atrophy (see Fig 3A), it might serve as an easily accessible and early peripheral blood readout for incipient central-nervous brain degeneration. Taken together, these findings do not merely confirm blood NfL as a biomarker altered already early in the course of genetic FTD,^{16,27} but provide a more fine-grained picture of its dynamics during the presymptomatic phase of the disease.

Moreover, our study now complements these findings on the dynamics of NfL with the dynamics of pNfH. It associates the onset of the pNfH increase with the onset of the symptomatic stage, as pNfH levels and pNfH change rates were increased in symptomatic, but not yet in presymptomatic or converting carriers. Correspondingly, modeling of the biomarker cascade showed that the pNfH increase occurred close to clinical onset. Thus, confirming and extending the earlier result of a cross-sectional piloting study,¹⁴ our study suggests that the pNfH increase might serve as a biomarker in the symptomatic phase of genetic FTD, paralleling findings from other multisystemic neurodegenerative diseases where pNfH increases were linked to later disease stages.²¹ Thus, the combination of both biomarkers – NfL and pNfH – might be clinically relevant in the early and late stages of neurodegenerative diseases.²⁸

Although neurofilament increases are specific in that they signal axonal decay rate (rather than merely unspecific cell damage), their value in genetic FTD does not primarily consist in their use as diagnostic biomarkers, as neurofilament levels are increased in various neurodegenerative and non-neurodegenerative conditions^{12,14,21,22,29–31} and as assessment of mutations and altered disease-specific proteins already meets such a diagnostic purpose.^{32–34} For preparing future FTD intervention trials, however, the biomarker value of neurofilament levels rather consists in their potential use as stratification, disease severity, and treatment response biomarkers. Particularly, our findings indicate that – as stratification biomarkers – neurofilament levels might allow demarcating

the conversion stage, for which the onset is marked by increased NfL levels and NfL change rates (but still normal pNfH levels) and its completion (with transition to the symptomatic stage) by increased pNfH levels. The combined use of NfL and pNfH levels as stratification biomarkers might thus help optimizing the selection of eligible mutation carriers for clinical trials, if one assumes that future disease-modifying therapies might be most effective in a window of opportunity immediately before clinical onset. Such fully biomarker-based stratification appears relevant as the age of onset in genetic FTD currently cannot be reliably predicted on the basis of the familial age of onset.^{17,35} NfL might even quantitatively capture proximity-to-onset as individual NfL levels of converters continuously increased with proximity to the individually observed clinical onset.

Neurofilament levels – and in particular NfL – might moreover serve as biomarkers of disease severity in the early phases of genetic FTD, as evidenced by their increase with increasing CDR plus NACC FTLD levels in these early phases. Whereas still normal at CDR stage 0, they progressively increase with the CDR stages 0.5 and >0.5. They then seem to reach a plateau, where these increased levels are maintained, indicating a stable rate of increased axonal decay at CDR stages >0.5 (see Figs 2C and 3A). Our findings thus expand and specify previous research reporting an association of NfL levels with FTD disease severity.³⁶ Moreover, our findings on the differential associations of NfL versus pNfH levels with upper versus lower motoneuron involvement (Supplement 3) – although still preliminary given the small sample size – are compatible with and extend previous findings suggesting that both NfL and pNfH correlate with the degree of clinical upper and lower motoneuron involvement,³⁷ but with pNfH levels correlating better with lower motoneuron affection and NfL levels better with upper motoneuron affection.^{37,38}

Our study provides first sample size estimates for future trials of disease-modifying treatments using neurofilament levels as treatment response biomarkers. Intra-individual biological variation is likely only a minimal source of noise when using neurofilament blood levels as outcome measure, as our study shows that levels of each NfL and pNfH are highly stable within individuals, as demonstrated by the high intraclass correlation coefficients in mutation carriers, assessed over ≈ 12 months (see Table 3), with biological stability not varying with age (Supplement 4). Using neurofilament levels as outcome parameters might thus help to reduce trial sample sizes in comparison to clinical outcome measures. Indeed, our sample size estimates for trials aiming to lower absolute NfL blood levels in genetic FTD indicate that a total

sample size of 12 subjects would suffice to detect therapeutic effect sizes of 50% (24 subjects for a more modest therapeutic effect size of 30%), if using NfL at the symptomatic stage. Importantly, our study demonstrates that the sample size estimates need to be stage-specific: If using NfL as outcome parameter at the conversion stage, a higher sample size of 18 subjects would be required for detecting the same therapeutic effect size, which is explained by quantitatively smaller increase of NfL levels at the conversion stage in comparison to the symptomatic stage.

Thus, whereas our findings show a higher sensitivity of NfL to capture the onset of the neurodegenerative process at the conversion stage, both analytes might be explored further in combination in future FTD natural history and treatment trials, given (1) the significant increase and high intraindividual stability of both NfL and pNfH, (2) their potential to demarcate the onset and the completion of the conversion phase, respectively, and (3) the possibility that they might yield differential responses and dynamics in response to therapeutic interventions or reflect different features of the disease process, as suggested for other neurodegenerative diseases.^{39–41}

Our study has several limitations. First, although we demonstrate that the later increase of pNfH relative to NfL levels is not due to differences in the technical and biological stability of both analytes, this effect might in part be explained by the smaller effect size of the pNfH increase. Therefore, further studies are warranted to scrutinize the differential cellular mechanisms and dynamics underlying NfL and pNfH increases in genetic FTD. A recent report already provides a first hint to an underlying biological difference: by the example of ALS, it suggests a metabolic shift from NfH expression to less energy consuming NfL expression in neurons of neurodegenerative disease patients.⁴² Such an altered metabolic profile of neurons exposed to neurodegeneration, with altered energy demands, might possibly explain the stage specific increase in NfL versus pNfH, which we observe here. Second, although the genetic subgroups of our study were sufficiently powered to confirm at least one of the main findings in each genetic subgroup (the increase of NfL and pNfH levels from the presymptomatic to the symptomatic stage, see Fig 1E and F), larger longitudinal cohort sizes per gene would be required to run such subgroup analyses also for the other findings, particularly for the key findings related to change rates, the converting subjects, and the temporal proximity of the biomarker changes to the hypothetical clinical onset. Although our study links the onset of the NfL increase clearly to the beginning of the conversion stage and the pNfH increase to the symptomatic stage of genetic FTD, first incipient

biological changes of pNfH levels during the conversion stage might possibly be captured with a substantially larger number of converters. Third, we used age as a proxy measure for the approaching symptom onset, like other studies, because no better proxy is currently available in genetic FTD and because the known high variation of onset age within families³⁵ would render analyses based on the average family onset age a possible source of uncertainty or bias. Fourth, the proposed preliminary biomarker cascade may require further gene-specific adjustments in larger genetic subcohorts, given the quantitative and qualitative differences observed here in the neurodegenerative process of each genetic group (see Fig 3B–D), also ideally integrating additional biomarker modalities into the cascade framework. Finally, our findings require validation in independent longitudinal genetic FTD cohorts, like the ALLFTD cohort.⁴³

In conclusion, our longitudinal study shows that blood NfL and pNfH provide stage-dependent stratification and, potentially, treatment response biomarkers in presymptomatic FTD, allowing demarcation of the conversion stage. The proposed preliminary biomarker cascade of NfL, pNfH, and volumetric MRI brain changes might help pave the way towards a biomarker-based precision medicine approach to genetic FTD, supporting the multimodal stratification of the presymptomatic phase.

Acknowledgments

The authors thank all participants and their families for their contribution to the GENFI study. C.W. and M.S. are members of the European Reference Network for Rare Neurological Diseases Project ID No. 739510. This work was supported by the Horizon 2020 research and innovation program (grant 779257 Solve-RD to M.S.), the National Ataxia Foundation (grant to C.W. and M.S.), the Wilhelm Vaillant Stiftung (grant to C.W.), the EU Joint Programme – Neurodegenerative Disease Research (JPND) “GENFI-prox” through participating national funding agencies (by DLR/BMBF to M.S., J.D.R., B.B., C.G., and M.O.), and the European Union’s Horizon 2020 research and innovation programme under grant agreement No. 643417. J.C.S. and H.S. received funding by two Memorabel grants from Deltaplan Dementie (The Netherlands Organisation for Health Research and Development and Alzheimer Nederland; grant numbers 733050813 and 733050103) in the Netherlands and the Bluefield Project to Cure Frontotemporal Dementia. J.B.R. was supported by the NIHR Cambridge Biomedical Research Centre (BRC-1215-20014) and the Medical Research Council (SUAG/051 G101400). C.B. is supported by a

postdoctoral fellowship from the Swiss National Science Foundation (P400PM_191077). J.D.R. is supported by the Miriam Marks Brain Research UK Senior Fellowship and has received funding from an MRC Clinician Scientist Fellowship (MR/M008525/1) and the NIHR Rare Disease Translational Research Collaboration (BRC149/NS/MH). This work was also supported by the MRC UK GENFI grant (MR/M023664/1), the Bluefield Project and the JPND GENFI-PROX grant (2019-02248). The funding sources had no role in the study design, data collection, data analysis, data interpretation, or writing of the manuscript.

Author Contributions

C.W., J.D.R., and M.S. contributed to the conception and design of the study. All authors contributed to the acquisition and analysis of data. C.W. and M.S. contributed to drafting the text and preparing the figures. The GENFI consortium authors and their affiliations are listed in a supplementary table (Supplement 5).

Potential Conflicts of Interest

Nothing to report by any of the authors.

References

- Rascovsky K, Hodges JR, Knopman D, et al. Sensitivity of revised diagnostic criteria for the behavioural variant of frontotemporal dementia. *Brain* 2011;134:2456–2477.
- Gorno-Tempini ML, Hillis AE, Weintraub S, et al. Classification of primary progressive aphasia and its variants. *Neurology* 2011;76:1006–1014.
- Greaves CV, Rohrer JD. An update on genetic frontotemporal dementia. *J Neurol* 2019;266:2075–2086.
- Hutton M, Lendon CL, Rizzo P, et al. Association of missense and 5'-splice-site mutations in tau with the inherited dementia FTDP-17. *Nature* 1998;393:702–705.
- Baker M, Mackenzie IR, Pickering-Brown SM, et al. Mutations in progranulin cause tau-negative frontotemporal dementia linked to chromosome 17. *Nature* 2006;442:916–919.
- Cruts M, Gijselink I, van der Zee J, et al. Null mutations in progranulin cause ubiquitin-positive frontotemporal dementia linked to chromosome 17q21. *Nature* 2006;442:920–924.
- Renton AE, Majounie E, Waite A, et al. A Hexanucleotide Repeat Expansion in C9ORF72 Is the Cause of Chromosome 9p21-Linked ALS-FTD. *Neuron* 2011;72:257–268.
- DeJesus-Hernandez M, Mackenzie IR, Boeve BF, et al. Expanded GGGGCC hexanucleotide repeat in noncoding region of C9ORF72 causes chromosome 9p-linked FTD and ALS. *Neuron* 2011;72:245–256.
- Panza F, Lozupone M, Seripa D, et al. Development of disease-modifying drugs for frontotemporal dementia spectrum disorders. *Nat Rev Neurol* 2020;16:213–228.
- Liscic RM, Alberici A, Cairns NJ, et al. From basic research to the clinic: innovative therapies for ALS and FTD in the pipeline. *Mol Neurodegener* 2020;15:31.
- Benussi A, Alberici A, Samra K, et al. Revising the definition of pre-clinical and prodromal frontotemporal dementia. in preparation.
- Khalil M, Teunissen CE, Otto M, Piehl Fredrik, et al. Neurofilaments as biomarkers in neurological disorders. *Nat Rev Neurol*. 2018;14:577–589. <https://doi.org/10.1038/s41582-018-0058-z>
- Kuhle J, Barro C, Andreasson U, et al. Comparison of three analytical platforms for quantification of the neurofilament light chain in blood samples: ELISA, electrochemiluminescence immunoassay and Simoa. *Clin Chem Lab Med* 2016;54:1655–1661.
- Wilke C, Pujol-Calderon F, Barro C, et al. Correlations between serum and CSF pNfH levels in ALS, FTD and controls: a comparison of three analytical approaches. *Clin Chem Lab Med* 2019;57:1556–1564.
- Wilke C, Preische O, Deuschle C, et al. Neurofilament light chain in FTD is elevated not only in cerebrospinal fluid, but also in serum. *J Neurol Neurosurg Psychiatry* 2016;87:1270–1272.
- van der Ende EL, Meeter LH, Poos JM, et al. Serum neurofilament light chain in genetic frontotemporal dementia: a longitudinal, multi-centre cohort study. *Lancet Neurol* 2019;18:1103–1111.
- Rohrer JD, Nicholas JM, Cash DM, et al. Presymptomatic cognitive and neuroanatomical changes in genetic frontotemporal dementia in the Genetic Frontotemporal dementia Initiative (GENFI) study: a cross-sectional analysis. *Lancet Neurol* 2015;14:253–262.
- Brooks BR, Miller RG, Swash M, et al. El Escorial revisited: revised criteria for the diagnosis of amyotrophic lateral sclerosis. *Amyotroph Lateral Scler Other Motor Neuron Disord* 2000;1:293–299.
- Miyagawa T, Brushaber D, Syrjanen J, et al. Use of the CDR[®] plus NACC FTLD in mild FTLD: Data from the ARTFL/LEFFTDS consortium. *Alzheimers Dement* 2020;16:79–90.
- Khalil M, Pirpamer L, Hofer E, et al. Serum neurofilament light levels in normal aging and their association with morphologic brain changes. *Nat Commun* 2020;11:812.
- Wilke C, Haas E, Reetz K, et al. Neurofilaments in spinocerebellar ataxia type 3: blood biomarkers at the preataxic and ataxic stage in humans and mice. *EMBO Mol Med* 2020 Jun 8;n/a(n/a);12:e11803.
- Wilke C, Dos Santos MCT, Schulte C, et al. Intra-individual neurofilament dynamics in serum mark the conversion to sporadic parkinson's disease. *Mov Disord* 2020;35:1233–1238.
- Bateman RJ, Xiong C, Benzinger TLS, et al. Clinical and Biomarker Changes in Dominantly Inherited Alzheimer's Disease. *N Engl J Med* 2012;367:795–804.
- Preischo O, Schultz SA, Apel A, et al. Serum neurofilament dynamics predicts neurodegeneration and clinical progression in presymptomatic Alzheimer's disease. *Nat Med* 2019 2019/02/01;25:277–283.
- Byrne LM, Rodrigues FB, Johnson EB, et al. Evaluation of mutant huntingtin and neurofilament proteins as potential markers in Huntington's disease. *Sci Transl Med* 2018;10:458.
- Jacobi H, du Montcel ST, Bauer P, et al. Long-term disease progression in spinocerebellar ataxia types 1, 2, 3, and 6: a longitudinal cohort study. *Lancet Neurol* 2015;14:1101–1108.
- Panman JL, Venkatraghavan V, van der Ende EL, et al. Modelling the cascade of biomarker changes in GRN-related frontotemporal dementia. *J Neurol Neurosurg Psychiatry* 2021;15:494–501.
- Barro C, Chitnis T, Weiner HL. Blood neurofilament light: a critical review of its application to neurologic disease. *Ann Clin Transl Neurol* 2020;7:2508–2523.
- Bridel C, van Wieringen WN, Zetterberg H, et al. Diagnostic value of cerebrospinal fluid neurofilament light protein in neurology: a systematic review and meta-analysis. *JAMA Neurol* 2019;76:1035–1048.
- Wilke C, Bender F, Hayer SN, et al. Serum neurofilament light is increased in multiple system atrophy of cerebellar type and in

- repeat-expansion spinocerebellar ataxias: a pilot study. *J Neurol* 2018;265:1618–1624.
31. Wilke C, Rattay TW, Hengel H, et al. Serum neurofilament light chain is increased in hereditary spastic paraplegias. *Ann Clin Transl Neurol* 2018;5:876–882.
 32. Ghidoni R, Benussi L, Glionna M, et al. Low plasma progranulin levels predict progranulin mutations in frontotemporal lobar degeneration. *Neurology* 2008;71:1235–1239.
 33. Finch N, Baker M, Crook R, et al. Plasma progranulin levels predict progranulin mutation status in frontotemporal dementia patients and asymptomatic family members. *Brain* 2009;132:583–591.
 34. Gendron TF, Chew J, Stankowski JN, et al. Poly(GP) proteins are a useful pharmacodynamic marker for C9ORF72-associated amyotrophic lateral sclerosis. *Sci Transl Med* 2017;9:9.
 35. Moore KM, Nicholas J, Grossman M, et al. Age at symptom onset and death and disease duration in genetic frontotemporal dementia: an international retrospective cohort study. *Lancet Neurol* 2020;19:145–156.
 36. Rohrer JD, Woollacott IO, Dick KM, et al. Serum neurofilament light chain protein is a measure of disease intensity in frontotemporal dementia. *Neurology* 2016;87:1329–1336.
 37. Poesen K, de Schaepdryver M, Stubendorff B, et al. Neurofilament markers for ALS correlate with extent of upper and lower motor neuron disease. *Neurology* 2017;88:2302–2309.
 38. Gille B, de Schaepdryver M, Goossens J, et al. Serum neurofilament light chain levels as a marker of upper motor neuron degeneration in patients with Amyotrophic Lateral Sclerosis. *Neuropathol Appl Neurobiol* 2019;45:291–304.
 39. Poesen K, Van Damme P. Diagnostic and Prognostic Performance of Neurofilaments in ALS. *Front Neurol* 2018;9:1167.
 40. de Vivo DC, Topaloglu H, Swoboda KJ, et al. Nusinersen in Infants Who Initiate Treatment in a Presymptomatic Stage of Spinal Muscular Atrophy (SMA): Interim Efficacy and Safety Results From the Phase 2 NURTURE Study (S25.001). *Neurology* 2019;92:S25.001.
 41. Winter B, Guenther R, Ludolph AC, et al. Neurofilaments and tau in CSF in an infant with SMA type 1 treated with nusinersen. *J Neurol Neurosurg Psychiatry* 2019;10:1068.2–1068.101069.
 42. Zucchi E, Lu CH, Cho Y, et al. A motor neuron strategy to save time and energy in neurodegeneration: adaptive protein stoichiometry. *J Neurochem* 2018;146:631–641.
 43. Rosen HJ, Boeve BF, Boxer AL. Tracking disease progression in familial and sporadic frontotemporal lobar degeneration: recent findings from ARTFL and LEFFFTDS. *Alzheimers Dement* 2020;16:71–78.
 44. Andreasson U, Perret-Liaudet A, van Waalwijk van Doorn LJ, et al. A practical guide to immunoassay method validation. *Front Neurol* 2015;6:179.